Structurally oriented coherent noise filtering

Geoffrey A. Dorn[1]* presents a novel post-stack structurally oriented coherent noise filter that removes footprint of any orientation and wavelength from a seismic volume.

Introduction

All seismic data, whether 2D, 3D, post-stack or pre-stack, contains noise. Typically, this noise is comprised of both coherent and random components. Coherent noise presents itself as regular patterns in the seismic data. It may appear to be random or coherent depending on the orientation of the slice on which it is being observed. For example, coherent noise associated with acquisition may appear random on vertical slices through the volume, with its coherent nature becoming apparent on horizontal slices through the volume.

When seismic data is processed, an effort is made to reduce the coherent noise in the seismic data by applying a variety of signal processing techniques. However, when the seismic volume is delivered to the client, it often includes remnant noise that processing was unable to remove without having a deleterious effect on the amplitudes and bandwidth of the seismic data.

Since the processed seismic volume typically contains coherent noise, managing that noise within an interpretation system is critical, as it has a significant negative impact on semi-automatic and automatic interpretation workflows and techniques including autotracking of horizons, imaging of faults and fractures, automatic extraction of faults, and interpretation of stratigraphy and geomorphology. An obvious example is the effect of noise on edge attributes (i.e., 'coherence' class attributes). Any noise in the seismic data, whether random or coherent, will appear as edges in the seismic attribute volume and may obscure the geologic features of interest in the edge attribute volume (faults, fractures, stratigraphy, and geomorphology).

Finally, many interpreters today must use older 3D seismic volumes, merged seismic volumes of a variety of acquisition designs and processing workflows. Even if the pre-stack data is still available, their company may not be in a position to spend the money required to re-process the data. Yet they still need and expect to be able to use modern advanced interpretation technology on the data.

In response to this need a post-stack structurally oriented coherent noise filtering process has been developed and is described, with an application to 3D seismic surveys from the North Sea. The results are evaluated by comparing seismic volumes, edge attribute volumes, and amplitude and phase spectra pre- and post-filtering.

Previous work on coherent noise filtering

There are many sources of random and coherent noise in 3D seismic volumes. Examples of sources include the environment in which data are being collected, the equipment used to collect the seismic data, the design of the 3D seismic survey, 'undesirable' seismic propagation effects, and processing artifacts. Detailed discussions of sources and effects of footprint in seismic data can be found in Chopra and Marfurt (2007) and in Yilmaz (2001).

Linear coherent noise in seismic data is frequently managed by using a combination of pre-stack and post-stack processes. Examples of these processes include dip filtering (Yilmaz, 2001), $k_x - k_y$ wavenumber filtering (Gulunay et al., 2006), f–k filtering (Chopra and Larson, 2000), and principal component filters (Done, 1999). Chopra and Marfurt (2014) present a very readable summary of pre- and post-stack coherent and random noise filtering from an interpreter's perspective.

Crawford and Medwedeff's footprint removal process

In 1999, an algorithm was proposed to remove linear coherent noise (also known as footprint) from horizontal slices through a 3D seismic volume (Crawford and Medwedeff, 1999).

As originally designed, the algorithm included the following assumptions:

- Each horizontal slice (time or depth slice) through the 3D seismic volume is treated as an image
- The coherent noise has the following characteristics:
  - It can be oriented in the inline or crossline directions
  - It is linear (i.e., not curved) when viewed on time or depth slices
  - It has an identifiable period or wavelength in the direction perpendicular to the linear feature.

Figure 1 shows a sketch of a 5 x 15 sample operator that might be used for a linear footprint with a wavelength of 5 samples. Each

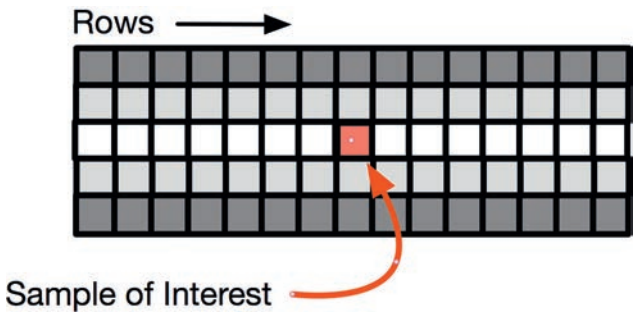

Figure 1 A 5-row by 15-column operator centred on the 'Sample of Interest' (shown in red), oriented to remove linear footprint parallel to the long dimension (Rows) in the operator. Grey levels indicate varying levels of seismic amplitude that define the footprint.

[1] CGG
* Corresponding author, E-mail: geoffrey.dorn@cgg.com

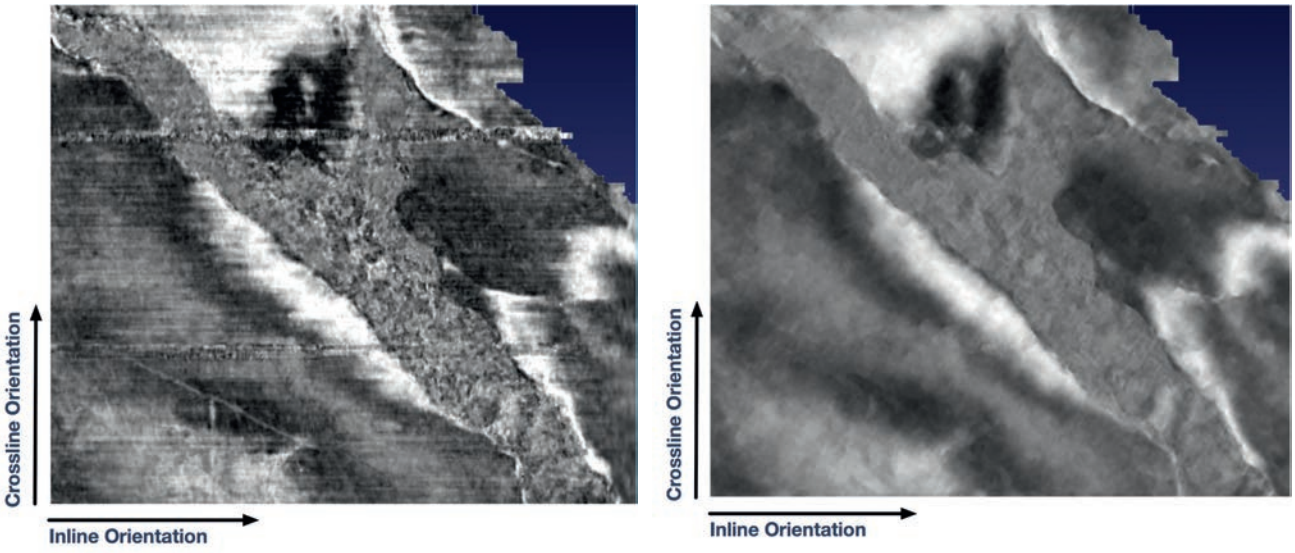

Figure 2 A horizontal slice at 380 ms from the K12 CD 3D seismic volume. Figure 2a is the slice prior to footprint removal, and Figure 2b is the slice after footprint removal.

'box' in the Figure represents a sample on the horizontal slice through the seismic volume. In a horizontally oriented operator as shown in Figure 1, the 'bins' in the operator coincide with the bins in the 3D seismic volume, and samples are located at the centres of the bins in (x,y). The grey levels are intended to illustrate the periodicity or wavelength of the footprint in the direction perpendicular to the trend of the footprint (referred to as the footprint orientation).

Definitions:

Operator Dimensions:

Number of rows = $2n+1$ (must be an odd number)

Number of columns = $2m+1$ (must be an odd number)

Operator Indices:

Row index: $-n \le i \le n$

Column index: $-m \le j \le m$

$V_{i,j}$ = Voxel (sample) value at position *i,j* in the operator

$V_{0,0}$ = Input voxel value at the voxel of interest (centre point of the operator shown in Figure 1 in red)

$V_{0,0}^{'}$ = Candidate new voxel value at the voxel of interest (centre point of the operator shown in Figure 1 in red)

$V_{0,0}^{o}$ = Output voxel value at the voxel of interest (centre point of the operator shown in Figure 1 in red)

Equations that describe Crawford and Medwedeff's implementation:

$$V_i^{MN} = \sum_{j=-m}^{m} V_{i,j} / (2m+1)$$

$$V^{MD} = Median\,|_{i=-n}^{n}\, V_i^{MN}$$

$$V_{0,0}^{'} = (V_{0,0} - V_i^{MN}) + V^{MD}$$

$$V_{0,0}^{o} = V_{0,0}^{'}$$

Figure 2a shows a portion of a time slice at 380 ms through the K12 CD survey, which covers portions of Blocks C and D, offshore Netherlands. The survey was acquired and processed around 1987-1988 as part of an exploration programme focused on gas reservoirs in the Rotliegende just below the Zechstein salt. The acquisition programme used streamers, but was narrow-azimuth and did not have the long offsets of modern 3D seismic volumes. The data was processed to 12.5 x 25 metre bins and was post-stack time-migrated and consisted of 998 crosslines, 394 inlines and extended from 0-4 s with a 4 ms sample rate.

K12 CD was chosen as an example of inline and crossline footprint. Along with some volumes from the Gulf of Mexico US continental shelf, this volume was among the surveys that motivated Crawford and Medwedeff's work on coherent noise filtering. It also includes some oblique coherent noise at depth.

The shallow portion of the volume includes a strong footprint in the inline direction and a weaker footprint in the crossline direction. Figure 2b shows the same slice after applying this footprint removal algorithm with the inline and crossline footprint wavelengths observed on time slices in the seismic volume. Footprint is significantly diminished after application of the above algorithm with appropriate wavelengths for both the inline and crossline footprint observable in Figure 2a. Note that the inline and crossline footprint has been removed from the data without disturbing the patterns in the underlying seismic signal on the slice.

The algorithm proposed by Crawford and Medwedeff has the following characteristics:

- It removes a single orientation and wavelength of footprint on each pass
- It preserves edges in the data so long as the edges do not occur with both the orientation and the wavelength corresponding to the orientation and wavelength of the footprint (i.e., it preserves geologic edges)
- It is data adaptive in that it will only remove footprint of the specified orientation and wavelength in the data where that footprint exists. Where that footprint is not present in the data, the effect of the algorithm is minimal.

Limitations of the original process

Applying this process on a variety of 3D seismic volumes has resulted in the recognition of a number of limitations of the

original process. Additions to and modifications of the original algorithm presented in this paper have effectively addressed these limitations. These modifications were integrated into the footprint removal process from 2010 through 2016.

Amplitude preservation

The primary goal of this Footprint Removal process is to remove coherent noise in such a manner that edges associated with the coherent noise are eliminated. This improves the imaging of edges associated with faults, fractures and stratigraphy in the seismic volume, which aids in the interpretation of these geologic features.

A secondary goal of Footprint Removal is to preserve amplitude information associated with lithology and fluid variations in the seismic data. The original algorithm took a first step toward preserving this information in the amplitude variation by being data adaptive (i.e., removing footprint where it was present and to the degree in which it was present, but affecting the data minimally where the specified footprint was not present). However, it overlooked two amplitude-related issues:

- The preservation of relative amplitude variations between slices, and
- The preservation of subtle relative amplitude variations laterally within slices.

Preservation of relative amplitude variations between slices vertically is accomplished through a combination of structurally orienting the footprint removal operator (which is discussed later in this paper), followed by applying a slice-specific gain factor to all of the sample amplitudes in each slice, such that each slice has the same Root Mean Square (RMS) amplitude after footprint removal as it had prior to footprint removal.

Small higher spatial frequency relative amplitude variations within a slice are preserved by setting a threshold value (ε) representing the minimum allowed percentage change between the input value and the raw output value at each voxel on the slice. If the percentage change is less than ε, then the original sample value is not changed.

Oblique footprint orientation

Footprint orientation and wavelength depends on the acquisition design, fold variations in acquisition, dead trace patterns, and a variety of other factors that can affect footprint in the final processed seismic volume. In many cases, linear footprint patterns are aligned with the inline direction, the crossline direction, or both. Unfortunately, there are often footprint patterns in the data that have oblique orientations relative to the inline and crossline axes of the 3D survey.

Figure 3a shows a horizontal slice at 1412 ms in the K12 CD 3D seismic volume. This image shows a number of footprint orientations. Some orientations are parallel to the inline direction, while several footprint orientations are oblique to the inline and crossline directions. An example of inline-oriented footprint is highlighted by a red arrow, while examples of oblique footprint orientations are highlighted by yellow arrows.

In order to implement the removal of oblique footprint, the operator illustrated in Figure 1 is centred at each voxel in the slice and is oriented with its long axis parallel to the specified orientation of the footprint. The width of the operator is set to be equal to the observed wavelength of the footprint (measured in traces). In an oblique orientation, the gridding of the cells in the operator is generally not aligned with the gridding of the voxels (samples) on each slice. Gridding of the samples on the slice is oriented parallel to the survey inline and crossline directions. As a result, the data samples that are available from the seismic volume are not positioned in the centres of the cells in the operator.

In order to obtain data values at the centre of each operator cell, the data on the slice is interpolated from the nearest neighbouring traces to the filter operator cell centre positions. Any 2D interpolation algorithm could be used for this step. In this example, bi-linear interpolation was used. Once data has been interpolated to the operator cell centres, the data in the operator is used as described above.

Figure 3a shows a time slice of the K12 CD seismic volume at 1412 ms prior to footprint removal. Figure 3b shows the same slice after applying the above footprint removal algorithm with

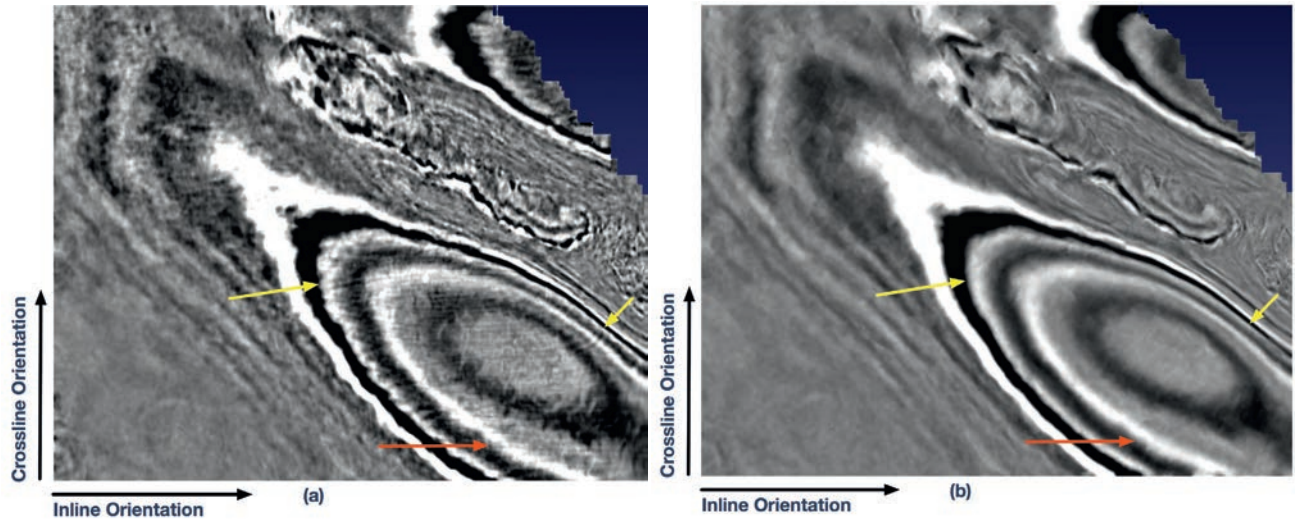

Figure 3 A time-slice from the K12 CD survey exhibiting inline (red arrow) and oblique (yellow arrows) footprint patterns. Figure 3a shows the slice prior to footprint removal. Figure 3b shows the slice after removal of the inline and oblique footprint.

the inline, crossline and oblique orientations and wavelengths measured from horizontal slices in the original seismic volume. The yellow arrows are pointing at and are oriented in the direction of oblique footprint, and the red arrow is pointing at inline footprint striping on the slice prior to footprint removal (Figure 3a) and the footprint has been eliminated after Footprint Removal has been applied (Figure 3b). Note that the footprint has been removed from the data without disturbing the patterns in the underlying seismic signal on the slice.

One of the noticeable differences between the shallow slice in Figure 2 and the deeper slice in Figure 3 is that with depth, the reflections are more steeply dipping. Dealing correctly with dipping reflectors requires that the Footprint Removal operator be structurally oriented.

Structurally oriented footprint removal

The footprint removal process described in the previous section of this paper uses a planar operator that is oriented to be horizontal. This approach has two potential problems:

1. Suppose that the intersection of dipping reflectors and the spacing between reflectors is such that the intersections of the peaks and troughs with the horizontal time or depth slices has a strike in the direction of the specified azimuthal orientation of the footprint. Let us also presume that the dipping reflections have an apparent wavelength that is equal to the wavelength specified for the footprint. In this situation, reflections might be removed from the volume as if they were footprint. This can occur when the footprint has been identified on a shallower slice (where footprint is more visible in the data), and where reflecting surfaces deeper in the volume have steep dip. Although this circumstance is relatively rare, it does occur.
2. Using a horizontal filter operator on time or depth slices mixes amplitude information from different reflections in the calculation of the amplitude correction to eliminate the specified footprint. This may occur if the horizontal operator is crossing multiple dipping reflections. Although the visible footprint is reduced or removed, the actual amplitudes might be compromised for subsequent quantitative application of seismic amplitudes to impedance inversion.

Problems similar to these have been encountered with other spatial filters applied to seismic volumes (Chopra and Marfurt, 2007). An estimate of local vector dip to orient the planar filter operator to dipping seismic reflectors has been used to improve the results of a number of spatial filters and processes, including random noise filtering and edge attribute calculations. Orientation of spatial operators to local dip is commonly called 'structurally oriented filtering'. Operator sizes for coherent noise filtering are somewhat greater than operators for these other applications. For example, a wavelength 5 coherent noise filter might have dimensions of 5 x 15 traces, while a random noise filter operator might be 5 x 5 traces. As a result, the orientation to local dip is even more critical in order to optimize the results of this coherent noise filter than it is for optimizing the results of a random noise filter such as a median or mean filter.

To illustrate, let the Cartesian co-ordinates of the data volume be (x,y,z) and let the Cartesian coordinates of the 2D operator grid be (u,v,w), where w = 0 (i.e., the operator is a 2D grid in the (u,v) plane). If an operator such as that shown in Figure 1 is oriented by rotation in the horizontal plane to the observed azimuth of the footprint, and subsequently also oriented to be perpendicular to the local 3D dip vector at the centre sample in the operator, the samples in the seismic volume will generally not be located at the 'bin' centres on the oriented operator either horizontally or vertically. In order to obtain sample values at the 'bin' centres of the dipping filter operator, the data need to be interpolated in 3D. In the remainder of this paper, the author uses 'footprint removal' to refer to generic footprint removal processing, and uses 'Footprint Removal' to refer to the specific structurally oriented footprint removal process described in this paper.

Application to attribute volumes and other geophysical data

The coherent noise (footprint) filter described in this paper can also be applied to attributes of seismic data (e.g., an edge attribute, spectral decomposition, or other attribute volumes). It may also be used to remove linear footprint from data volumes that have been derived from other physical modalities (e.g., gravity, magnetic or electromagnetic data).

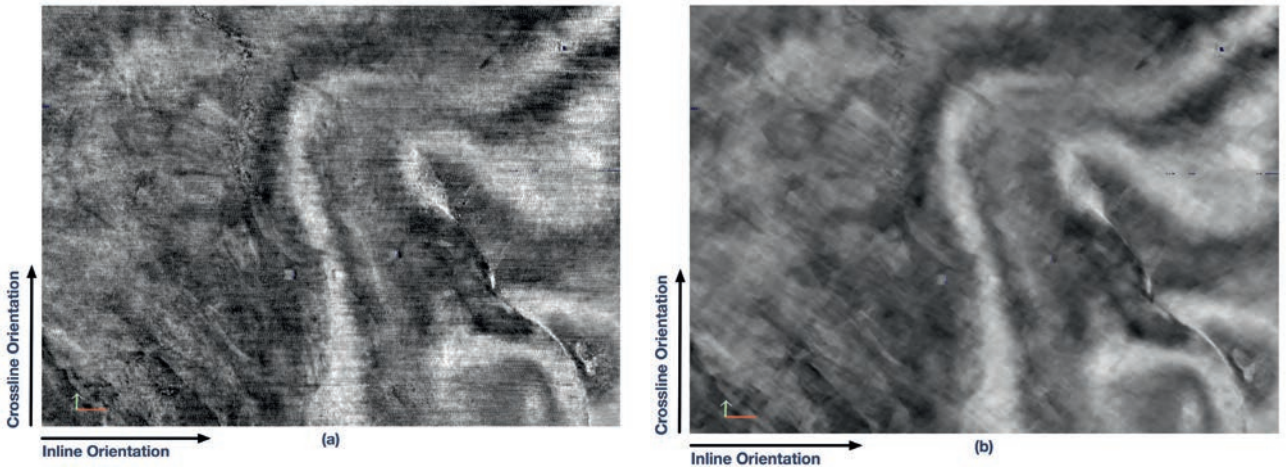

Figure 4 A portion of a time-slice from the F3 survey exhibiting inline and oblique footprint patterns. Figure 4a shows the slice prior to footprint removal. Figure 4b shows the slice after removal of the inline and oblique footprint.

Iteration	Orientation (Degrees from North)	Wavelength (Bins)	Iteration	Orientation (Degrees from North)	Wavelength (Bins)
1	0	3	12	38	3
2	90	3	13	14	3
3	0	5	14	48	3
4	90	5	15	144	3
5	0	11	16	127	3
6	90	11	17	9	3
7	20	3	18	70	3
8	155	7	19	58	3
9	90	13	20	30	3
10	157	11	21	107	3
11	163	3			

Table 1 Footprint orientations and wavelengths.

Application to the F3 volume from the North Sea

The F3 Block data is from the southern North Sea, offshore Netherlands. The area is located to the northeast of the K12 CD survey. The acquisition of the F3 survey was approximately contemporaneous with the K12 CD survey (1987). The survey consists of 650 inlines, 950 crosslines and ranges from 0 to 1848 ms (4 ms sample rate). (The original volume likely extended to 4 s in time, like the K12 CD survey, but was truncated approximately at the Top Rotliegende/Base Zechstein interface (1848 ms) prior to making the survey publicly available).

Acquisition and processing for this survey are similar to those used for K12 CD. Data was acquired using streamers, the data is not wide azimuth, and the offsets are shorter than for more modern surveys. The data was post-stack time-migrated. Like the K12 CD volume, there remains quite a bit of footprint in the processed volume.

Table 1 lists each of the 21 different footprint orientation/wavelength combinations that were identified by examining six different time-slices in the first 1.5 seconds of data in the volume. The survey orientation is such that crosslines have an orientation of 0^o (north-south), and inlines have an orientation of 90^o (East-West).

A set of 21 different footprint wavelength/orientation pairs is not something that is observed all at once. Typically the user starts on a shallow time/depth slice and identifies an initial set of 3-5 footprints. These are filtered out in one application of the footprint removal process. Once those orientation/wavelength pairs have been removed from the data, it will be possible to see additional footprint wavelengths and orientations that were previously obscured by the first 3-5 footprints. As this workflow continues, the interpreter should also examine time/depth slices deeper in the volume. Proceeding in this fashion, the typical survey will have between 7 and 20 footprints to removed. The maximum number of footprints that have been removed from one survey, during the five years or so that this technology has been in use, is more than 40. The maximum footprint wavelength that has been removed over that same period of time is 45 traces.

The Footprint Removal process is computationally intensive. At every sample in the seismic volume, the data values are interpolated in 3D to the bin centres of an operator that is oriented by both the footprint azimuth and by the local structural dip vector. The structural dip volume must also be recalculated after each footprint has been removed from the seismic data. This is necessary because the footprint in the volume affects the calculated values of structural dip. If a structural dip volume is re-used for a later Footprint Removal, the presence of footprint in the structural dip volume (i.e., footprint that has already been removed from the amplitude volume) means that Footprint Removal will simply reintroduce that footprint back into the amplitude volume while removing another footprint.

In order to achieve results in a relatively short period of time, the Footprint Removal process is implemented to run not only on the CPU cores in a workstation, but also on the GPU cores on the graphics cards. This makes several thousand processors available to perform the computation. The F3 survey has dimensions of 950 crosslines x 650 inlines x 463 time samples. As a floating-point volume, this is approximately 1.125 GB in size. The 21 footprint orientations/wavelengths were filtered from the F3 volume in 16 min and 15 seconds on a deskside workstation with a total of 5500 GPU cores, e.g., a workstation with two appropriately sized graphics cards installed.

The Footprint Removal process was applied to the F3 seismic volume and sequentially removed each of these observed footprint orientation/wavelength pairs. Figure 4 is a comparison of a portion of time slice 218 before (Figure 4a) and after (Figure 4b) Footprint Removal.

The structurally oriented Footprint Removal process effectively removes the footprint (inline, crossline and oblique orientations) revealing subtle NW-SE trending striations in the data that are associated with the geology, but that were previously obscured by the coherent noise. The histogram clipping levels in the display of the pre- and post-footprint removal time slices in Figure 4 are identical.

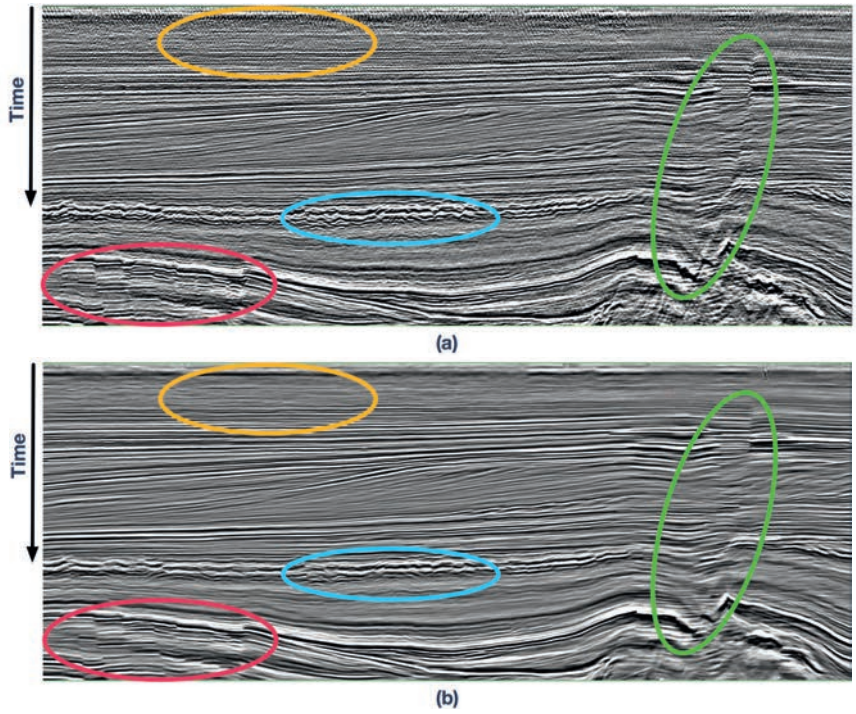

Figure 5 A portion of an inline from the F3 volume. Figure 5a shows the inline prior to Footprint Removal. Figure 5b shows the inline after removal of the inline and oblique footprint. The orange, red and green ovals highlight areas on the section that exhibit significant improvements in imaging horizons and faults after the footprint has been removed.

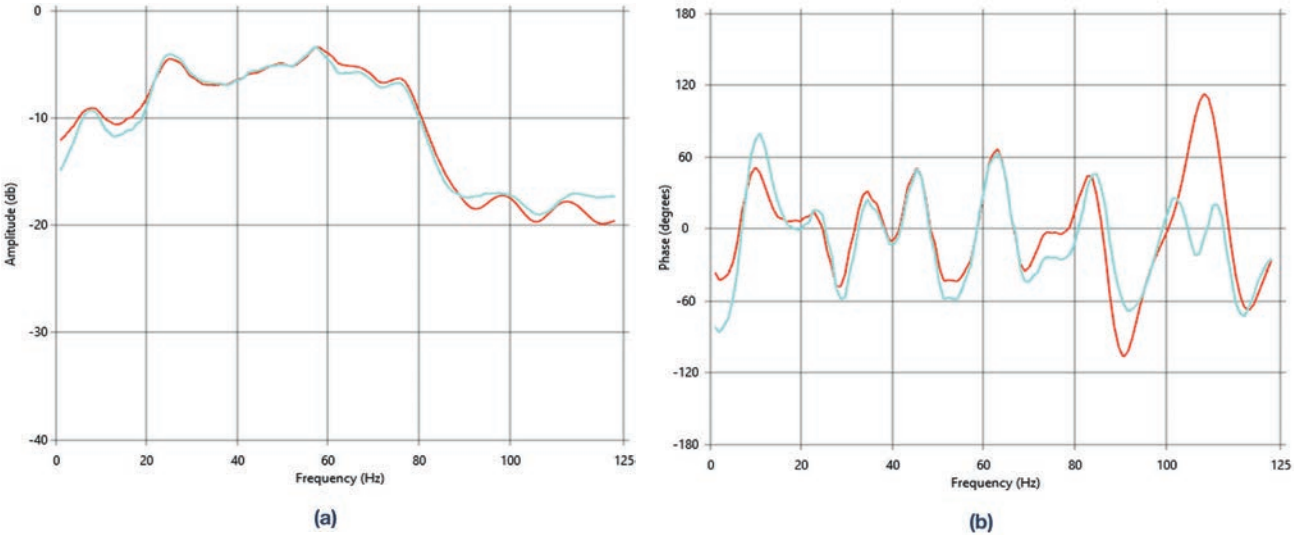

Figure 6 Average amplitude (Fig. 6a) and phase (Fig. 6b) spectra obtained in a 5x5 patch of traces in the centre of the F3 survey. The red line represents the average amplitude and phase spectra before footprint removal. The blue line represents the average amplitude and phase spectra after footprint removal.

Figure 5 shows a comparison of a portion of an inline before (Figure 5a) and after (Figure 5b) Footprint Removal. Close examination of the data in the orange oval in Figure 5a shows a substantial amount of noise in the shallow section that is associated with the various oblique footprint orientations with a wavelength of 3 in the volume. Comparing this with the data in the orange oval in Figure 5b shows that the short wavelength footprint has been removed by the Footprint Removal process.

The red oval highlights a portion of the section where there is the steep normal faulting which is characteristic of a hard-rock environment (in this case the Rotliegende). By comparing this region between Figures 5a and 5b, note that the crispness of the steeply dipping normal faults is retained after footprint removal has been applied to the volume. Some 'jitter' in the events in that interval associated with longer wavelength footprint in the volume has also been removed.

In the portion of the section within the green oval there are a couple of steeply dipping through-going faults, the top third of which contains an interval with bright amplitudes associated with a known gas reservoir. The imaging of the faults has been maintained or improved by the removal of footprint. Several steeply dipping noise artifacts in the bottom third of the green oval have also been filtered out of the volume.

Finally, the portion of the data within the blue oval is part of a de-watered shale that is widespread in the North Sea. In this part of the North Sea, the shale is quite thin, but some polygonal faulting is present in that interval. (Further to the north and west in the area around Balmoral and Blenheim fields in the UK waters, the interval of dewatered shale and polygonal faulting is much thicker.) The

primary effect of the footprint removal on the dewatered shale is the elimination of some minor noise in the reflections.

The elimination of coherent noise has substantially improved the quality of the seismic data. This should have a significant positive effect on manual and automated interpretation techniques, the quality of attribute volumes, and on impedance inversion and rock property determination.

Impact of footprint removal on the seismic bandwidth in the F3 Volume

Whenever a significant amount of filtering is applied to a volume, the interpreter must be concerned about the resulting bandwidth of the filtered volume. One of the primary purposes of structural orientation of the process is to minimize the effect of the filtering on the bandwidth of the data. Comparing the sharpness of the seismic reflections between Figures 5a and 5b (pre- and post-filtering) is encouraging, as the reflection events do not seem to be any broader vertically in Figure 5b than they were in Figure 5a before Footprint Removal was applied.

Figure 6 shows the average amplitude and phase spectra for a 5x5 patch of traces centered in the survey. The trace segments used in the spectral analysis extended from 200 ms to 1800 ms – a total of 400 samples. The average amplitude and phase spectra obtained on the data prior to Footprint Removal are shown in red. The average spectra obtained on the data after Footprint Removal are shown in light blue.

There is very little effect on either the amplitude or phase spectra in the effective bandwidth of the seismic data, which ranges from about 3 Hz to 85 Hz. This structurally oriented Footprint Removal algorithm has negligible effect on the spectral shape and bandwidth of the seismic volume. Spectral analyses were also carried out in the same location in the survey, with trace segments that were 128 samples in length and 256 samples in length. The average spectra for 128 sample and 256 sample trace segments exhibited the same minimal effect owing to footprint removal as the spectra associated with a trace length of 400 ms.

Impact of footprint removal on seismic attributes — edge attributes

Another key concern with regard to noise filtering is the effect that it has on edge imaging in the seismic volume. The dimensions of the operator for Footprint Removal are based on the wavelength of the footprint to be removed. Since the aspect ratio of the operator for Footprint Removal is typically between 1 and 3, a wavelength of 11 samples is filtered out by using an operator that has dimensions between 11 x 11 (aspect ratio of 1) to 11 x 33 (aspect ratio of 3). Given potentially large operator dimensions, does Footprint Removal filter out the noise while preserving the sharpness of the geologic edges in the seismic volume?

Figure 7 shows the results of calculating a structurally oriented edge or coherence class attribute called Horizon Edge Stacking (HES) in InsightEarth (Dorn and Kadlec, 2011) on the unfiltered seismic volume (Figure 7a) and on the volume with the footprint removed (Figure 7b). The data shown in Figure 7 is from the same seismic inline as was shown previously in Figures 5a and 5b. The histogram clipping on the data in Figure 7a and 7b is identical.

The overall appearance of the HES attribute in Figure 7a is very noisy. Most of that noise has been suppressed by applying footprint removal to the input seismic volume, resulting in a much cleaner HES attribute (Figure 7b). In the red oval in the lower left corner of Figures 7a and 7b, there are several steeply dipping faults in the Cretaceous section. Although these faults are imaged in both HES volumes, the surrounding background noise is weaker (e.g., is not as dark) after Footprint Removal has been applied. The blue oval in Figures 7a and 7b highlights a portion of a dewatered shale interval that has extensive polygonal faulting. The noise in the HES volume that was created before Footprint

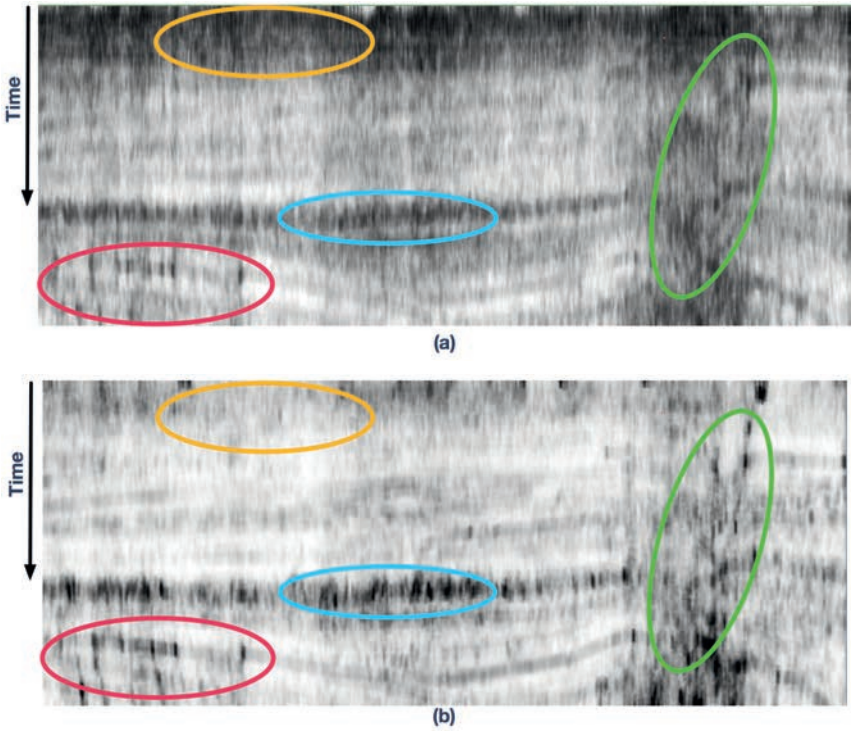

Figure 7 A portion of an inline from the F3 volume. Figure 7a shows the HES edge attribute calculated on the volume without Footprint Removal. Figure 7b shows the HES edge attribute calculated on the volume after footprint removal has been applied. The orange, red, green and blue ovals highlight corresponding areas on the section that exhibit significant improvements in imaging faults after the footprint has been removed.

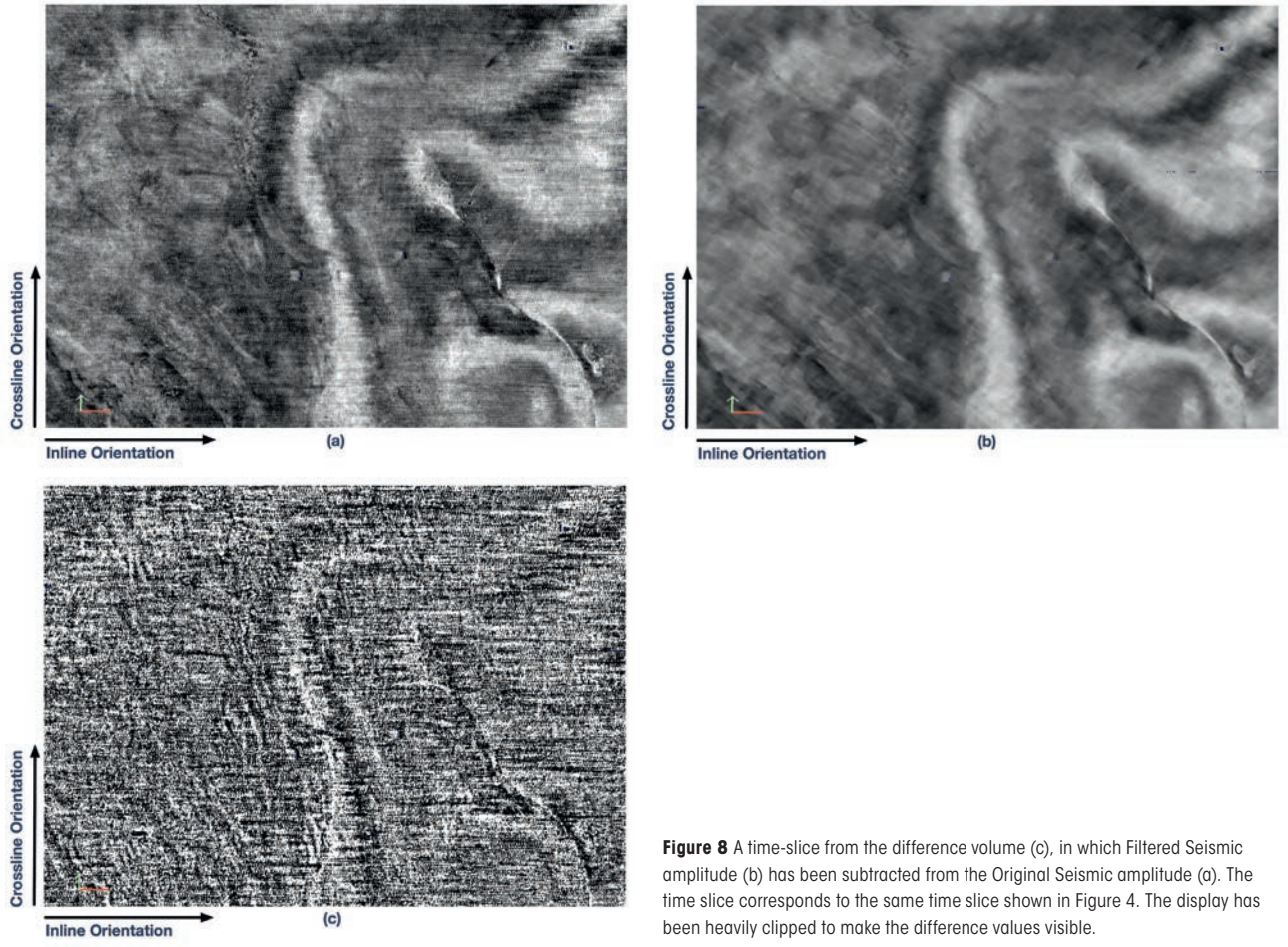

Figure 8 A time-slice from the difference volume (c), in which Filtered Seismic amplitude (b) has been subtracted from the Original Seismic amplitude (a). The time slice corresponds to the same time slice shown in Figure 4. The display has been heavily clipped to make the difference values visible.

Removal was applied results in a swath of discontinuous edge values throughout the shale interval. When applied to the Footprint-Removed volume, the HES attribute volume (Figure 7b) images individual faults within the thin shale interval. The green oval in Figures 7a and 7b highlights a large through-going fault in the HES data calculated after Footprint Removal (Figure 7b). In the HES data that was calculated without Footprint Removal (Figure 7a), the through-going fault is obscured by noise. Within the orange oval in the shallow seismic section there is very little discontinuity in the data (Figure 7b) after Footprint Removal, whereas before Footprint Removal the shallow section in the orange oval appears to be one large discontinuity (Figure 7a).

Difference volumes — visualizing the noise filtered from the volume

One final check on the Footprint Removal process is to calculate a difference volume between the original seismic volume and the filtered seismic volume. With random noise filtering, the difference volume should have a very 'random' appearance with little or no seismic structure exhibited on sections and time/depth slices through the difference volume.

Coherent noise that is linear on a horizontal slice in the seismic volume is present in the form of alternating stripes of brighter and darker data in the seismic image (assuming the data is displayed in a variable intensity colour scale). For example, in Figures 2a, 3a and 4a the footprint is visible as linear stripes of varying brightness in the respective colour scales. The footprint is visible because there is a somewhat stronger amplitude in one stripe and a somewhat weaker amplitude in the neighboring stripe.

Footprint Removal is simply a process that adjusts the amplitudes in the neighbouring stripes so that the brightness in neighboring stripes is approximately the same. If the gain is boosted in one stripe and reduced in another stripe, the difference volume on horizontal slices should have a striped appearance, which simply shows how much the local 'gain' had to be adjusted to achieve an elimination of the stripes in the seismic volume.

Figure 8c shows a time slice from the difference volume for the F3 survey, chosen at the same time as the slices in Figure 4a and 4b, (which are reproduced here as Figures 8a and 8b). The data displayed is the arithmetic difference between the unfiltered slice in Figure 4a and the filtered slice in Figure 4b. Figure 8c shows striping of varying orientations and wavelengths, as expected.

There is some apparent reflection structure in the difference volume, because the amplitude adjustment required to eliminate the footprint will typically be larger where the seismic amplitudes are stronger, and the adjustments will typically be smaller where the seismic amplitudes are weaker. For the same reason, if the vertical inline slice is taken through a difference volume and is centered on a footprint stripe that is oriented in the inline direction, there will be apparent structure in the vertical section at levels in the data that have that footprint present in the unfiltered seismic volume.

Conclusions

Linear coherent noise, or footprint, has been and remains a problem in stacked migrated 3D seismic volumes. It is critical to remove this noise from the volumes in order to rapidly and accurately interpret the seismic volumes. Modern methods of interpretation such as autotrackers, fault and fracture imaging attributes, RGB blending of spectral decomposition volumes, stratal transforms, and many other tools of interpretation will provide significantly better results and performance after the footprint is removed from the seismic volume.

A structurally oriented Footprint Removal process has been developed from an original concept suggested in 1999 based on a statistical de-striping algorithm. This Footprint Removal process is edge-preserving, data adaptive, amplitude and phase preserving, and structurally oriented. It can remove any orientation and wavelength of footprint that is present in the data. It removes footprint while retaining the more subtle variations in seismic amplitudes associated with geologic variations. By removing the footprint at the beginning of the interpretation workflow, Footprint Removal improves the results produced by edge imaging attributes, and any other attribute created from the seismic data.

Acknowledgements

I would like to thank CGG for permission to publish this paper. I would also like to acknowledge the Open Seismic Repository (OSR) and its website maintained by dGB Earth Sciences from which the F3 dataset can be downloaded. I would also like to thank ARCO's management for providing permission many years ago to publish work performed on the K12 CD survey. All data display and interpretation was performed using CGG GeoSoftware's InsightEarth advanced seismic interpretation software package.

References

Chopra, S. and Marfurt, K.J. [2007]. Seismic Attributes for Prospect Identification and Reservoir Characterization. SEG Geophysical Developments Series No. **11**, 464 pp.

Chopra, S. and Marfurt, K.J. [2014]. Causes and appearance of noise in seismic data volumes. *AAPG Explorer*, **35** (3), 52-55, 59.

Chopra, S. and Larson, G. [2000]. Acquisition footprint – Its detection and removal. *CSEG Recorder*, **25** (8), 16-20

Crawford, M. and Medwedeff, D. [1999]. *Automated extraction of fault surfaces from 3-D seismic prospecting data.* US Patent No. 5,987,388.

Dorn, G. and Kadlec, B. [2011]. Automatic fault extraction in hard and soft rock environments. *SEPM Society for Sedimentary Geology*, **31** (12).

Gulunay, N., Benjamin, N. and Magesan, M. [2006]. Acquisition footprint suppression on 3D land surveys. *First Break*, **24** (2), 71 – 77.

Done, W. J. [1999]. Removal of interference patterns in seismic gathers, In: Kirlin, R. L. and Done, W.J. (Eds.) *Covariance analysis for seismic signal processing.* Society of Exploration Geophysicists, Geophysical Developments, **8**, 185-225.

Yilmaz, O. [2001]. Seismic data analysis: Processing, inversion and interpretation of seismic data. Society of Exploration Geophysicists. *Investigations in Geophysics*, **10**, (1) 837 - 976.